

HDRVideo-GAN: Deep Generative HDR Video Reconstruction

Mrinal Anand*

Indian Institute of Technology
Gandhinagar, Gujarat, India
mrinal.anand@iitgn.ac.in

Chandan Kumar*

Indian Institute of Technology
Gandhinagar, Gujarat, India
chandan.kumar@alumni.iitgn.ac.in

Nidhin Harilal*

University of Colorado
Boulder, Colorado, USA
nidhin.harilal@colorado.edu

Shanmuganathan Raman

Indian Institute of Technology
Gandhinagar, Gujarat, India
shanmuga@iitgn.ac.in

ABSTRACT

High dynamic range (HDR) videos provide a more visually realistic experience than the standard low dynamic range (LDR) videos. Despite having significant progress in HDR imaging, it is still a challenging task to capture high-quality HDR video with a conventional off-the-shelf camera. Existing approaches rely entirely on using dense optical flow between the neighboring LDR sequences to reconstruct an HDR frame. However, they lead to inconsistencies in color and exposure over time when applied to alternating exposures with noisy frames. In this paper, we propose an end-to-end GAN-based framework for HDR video reconstruction from LDR sequences with alternating exposures. We first extract clean LDR frames from noisy LDR video with alternating exposures with a denoising network trained in a self-supervised setting. Using optical flow, we then align the neighboring alternating-exposure frames to a reference frame and then reconstruct high-quality HDR frames in a complete adversarial setting. To further improve the robustness and quality of generated frames, we incorporate temporal stability-based regularization term along with content and style-based losses in the cost function during the training procedure. Experimental results demonstrate that our framework achieves state-of-the-art performance and generates superior quality HDR frames of a video over the existing methods.

CCS CONCEPTS

• **Computing methodologies** → **Computational photography**;
Image-based rendering.

KEYWORDS

Computational Photography, HDR Video Reconstruction, GAN, Adversarial Training, Self-Supervised Training

1 INTRODUCTION

The dynamic range that the human visual system can experience in the real world is vast. Unfortunately, most off-the-shelf digital cameras capture only a limited range of illumination in the scene. This discrepancy has led to a great deal of research in reconstructing still HDR images from the conventional LDR off-the-shelf camera images. Most of these works have used a bracketed exposure imaging method [4, 18, 32, 33] which involves taking multiple images at different exposures and merging them to generate a single HDR image.

Generating HDR images by taking multiple images with different exposures may involve object/ camera movement. Therefore these methods end up producing ghosting artifacts in dynamic scenes of the image. These artifacts can be reduced through various methods like replacing/rejecting the pixels that move across the images [22, 54, 57], merging all different exposure images with a reference image [9, 50, 51] or aligning and reconstructing in a unified optimization system [45, 57]. Capturing HDR video directly involves expensive specialized cameras that use complex optical systems [48], and sensors [56].

On the other hand, reconstructing HDR video from the LDR sequence obtained from a standard off-the-shelf camera is a much more challenging task. Existing methods that are focused on reconstructing HDR images have been observed to generate temporally unstable results when applied to video sequences.

There exist few works addressing this problem [20, 21, 27, 31], which are typically slow and have limitations in several scenarios. Recently, the first deep learning-based approach was proposed by Kalantari *et al.* [19] for HDR video reconstruction, which utilized dense frame-to-frame motion information (optical flow) [29]. Their method first aligns the neighboring alternating exposure LDR frames to a reference frame by computing the optical flow between them, and then they use a convolutional neural network (CNN) based model to merge and reconstruct the final HDR frame. Although they show a reduction in time while reconstructing the HDR frames by a certain factor but as pointed out by its authors, their approach still suffers from discoloration and flickering artifacts in the reconstructed HDR video frames.

In this paper, we take inspiration from [19] and design a Generative Adversarial Network (GAN) based framework for reconstructing HDR video frames from the LDR sequence with alternating exposures. Kalantari *et al.* [19] performed an end-to-end training by minimizing the error between the reconstructed and ground truth HDR video frames on a set of training scenes. We show that merely reducing the pixel to pixel error between reconstructed and ground truth HDR frames from noisy LDR is prone to content loss and undesirable artifacts in the generated frames. We address this by proposing a framework comprising of an LDR denoising network, a light-weight optical flow estimation network, and a GAN based model for final HDR reconstruction. We modify the training procedure of our GAN based model by incorporating a temporal-stability based regularization term [6] along with content and style-based losses in the cost function while training the network. We use an

*denotes equal contribution

altered version of an existing optical flow estimation model, LiteFlowNet [14], which is fine-tuned to estimate the dense optical flow between LDR frames with varying exposures. The estimated optical flow is then used to align the LDR frames with alternating exposures to the current frame. The final HDR frame is generated by using a Generative Adversarial Network (GAN). In addition to the regularization term, standard adversarial loss, and the HDR reconstruction losses, we also incorporate perceptual loss [17], and style-aware content loss [43] while training the network for better performance. The proposed framework generates temporally stable HDR video with high visual quality.

GAN based models require a lot of data for image synthesis tasks. For the HDR reconstruction, we generate our training dataset synthetically by extracting the input LDR frames from a set of open-sourced HDR video repositories [8, 24]. However, unlike these synthetically generated LDR videos, frames captured from standard digital cameras have varied noise in them. Therefore, for the framework to generalize well, we fuse the LDR frames with the Gaussian noise of varied signal-to-noise (SNR) ratios. The main contributions of our work are given below:

- We propose the first GAN-based method for the HDR video reconstruction by using LDR frames with alternating exposures. Our proposed framework consists of a denoising network for extracting clean LDR frames, a light-weight optical flow estimation network, and a GAN based model for final HDR reconstruction.
- We incorporate perceptual as well as style-aware content losses to improve the visual quality of HDR frames. Along with utilizing the optical flow, we also incorporate a temporal-stability based regularization while training to further reduce the temporal incoherence in the reconstructed HDR frames.
- Our experimental results on the different HDR video datasets demonstrate that the proposed framework outperforms the existing approaches and produces high-quality HDR video.

Outline of the paper: The entire paper is organized as follows. Section 2 narrates the related work in the area of HDR imaging. Section 3 describes the dataset used for the experimentation. Section 4 presents the model architecture in detail. Section 5 describes the details about the used hyperparameters. Section 6 reports the qualitative and quantitative evaluations against the baseline. Finally, section 7 presents the ablation study.

Notation	Description
L_i –	original i^{th} LDR frame (alternating expos.)
\hat{L}_i –	i^{th} generated clean LDR (alternating expos.)
\tilde{L}_i –	aligned i^{th} clean LDR (alternating expos.)
H_i –	Original i^{th} HDR frame
\tilde{H}_i –	Generated i^{th} HDR frame
T_i –	i^{th} Tonemapped Frame of original HDR
\tilde{T}_i –	i^{th} Tonemapped Frame of generated HDR

Table 1: Description of notations frequently occurring in the paper

2 RELATED WORK

In the last few years with the onset on learning algorithm, the problem of HDR imaging has also been extensively explored. However, a lot of work is centered around the generation of still HDR images. One set of approaches uses a sequence of different exposure images to generate HDR images [3, 13, 18, 30, 40, 45], while the other approach uses burst images to generate the HDR image [11, 28]. There are some more focused works in the last few years to generate HDR images from a single image [5, 36]. Almost all these approaches are not suitable for generating HDR video because of the lack of temporal consistency in still HDR imaging. For brevity, we will only discuss the works related to the generation of HDR video.

The system that produced the most high-quality results to date has been the specialized camera that directly captures HDR video. These cameras include special sensors that can capture extensive dynamic range [2, 39, 44] or the camera which has beam-splitters that deflects the light to many sensors such that ever sensors measure the different amount of radiance concurrently. However, these approaches are limited because they need specialized custom hardware that has enormous costs and, therefore, less widespread [23, 49].

One way to generate HDR video is from the input sequence of frames having alternate exposure of each frame. Kang *et al.* [21] first proposed the method of HDR video reconstruction using the alternating exposure LDR frames. They used optical flow to align the neighboring frames to the reference frame. After aligning the nearby frame to the reference frame, they take a weighted sum to combine with the reference frame to avoid ghosting artifacts. However, their approach leads to ghosting artifacts when the scene has a significant amount of motion.

Mangiant and Gibson [21] improved the approach of Kang *et al.* [21] using a block-based motion estimation method which was coupled with a refinement stage. In their successive work, they filtered the region with a significant motion to minimize the blocking artifacts. However, their approach still had the blocking artifacts when the scene has substantial movement in it. In addition to that, their approach is limited to working only on two exposure sequences. Kalantari *et al.* [20] propose a patch-based method to reconstruct the missing exposure at each frame. After reconstruction, all the images produced were combined to obtain the final HDR frame. Temporal coherency is improved by estimating the motion between the neighboring/adjacent and the reference frame. However, the patch search was constraint only to small window around the predicted movement, where a greedy approach obtains the window size. This method produces the result, which is significantly better than the previous approach. However, to solve the complex patch-based optimization was a time consuming process and produce a single HDR frame. A major drawback of this approach was that it often was unable to constrain the patch search properly and underestimates the search window size. Ghosting artifacts were observed in such cases. One further work is [10] that improves the method of Kalantari *et al.* [20] by adaptively adjusting the exposure. In a recent work by Li *et al.* [27] proposes to consider the HDR video reconstruction problem as a maximization of posteriori estimate. Their method focuses on finding the foreground and background of each HDR frame separately. They extract the background and

foreground using rank minimization and multiscale adaptive regression techniques, respectively. The major drawback of this method is also the computational cost involved, it takes around two hours to generate a single frame with 1280×720 resolution. Additionally, many of the frames were accompanied by noise and discoloration.

Recently, Kalantari and Ramamoorthi [19] have proposed an approach in which they have used two connected networks called Flow network and Merge Network. Flow Network aligns the neighboring frame with the current frame, while the Merge network is used to merge the aligned frames with the reference frame. Their approach solves the problem in the best way so far. This is also state of the art for HDR video generation. But there are still ghosting artifacts in the challenging cases where the reference image is overexposed or if there are notable parallax and occlusion.

3 DATASET

We require a large dataset consisting of HDR video frames with corresponding LDR frames having alternating exposures. We use two publicly available HDR video datasets curated by Froehlich *et al.* [8] (13 videos) and Kronander *et al.* [24] (8 videos). These datasets were prepared using cameras with a specific optical design containing external [8] and internal [24] beam filters. The dataset contains 41 HDR videos, out of which 38 were used for training, and the remaining three were used as the hold-out test set consistent with the current state-of-the-art method proposed by Kalantari *et al.* [19] during experiments. We generate synthetic LDR frames from ground truth HDR frames at different exposures using Eq 1.

$$L_i = g_i(H_i) = \text{clip}[(H_i t_i)^{1/\gamma}] \quad (1)$$

here γ is 2.2, H_i is HDR image in linear domain, t_i is the exposure time, and clip function clips the output in the range $[0, 1]$. Figure 1 shows the comparison of an underexposed, and overexposed LDR frames, along with an HDR frame. It can be clearly seen from Figure 1 (a) and (b) clearly depicts the content loss in overexposed and underexposed LDR frames as compared to the corresponding HDR.

4 PROPOSED ARCHITECTURE

In this section, we present a detailed discussion of our proposed framework. Our proposed framework consists of three parts, i.e., an LDR denoising network for extracting clean LDR frames from

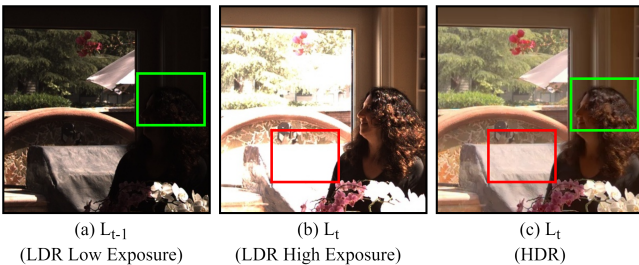


Figure 1: Visual comparison of the over and under exposed LDR frames generated using Equation 1 with the corresponding HDR frame. Note the loss of details in the dark and bright regions of under and over exposed LDR frames.

noisy LDR video, a lightweight optical flow estimation network, and a GAN based model for the final reconstruction of high-quality HDR frames.

Notations. Table 1 summarises all the variables used in this paper and their corresponding definitions. Here L denotes the LDR frame, H denotes the HDR frame, and T denotes the tonemapped HDR. An important point to note here is that i represents the i^{th} frame of the video. So $(i - 1)^{th}$ and $(i + 1)^{th}$ represents previous frame and the next frame with respect to the i^{th} frame.

4.1 Self-Supervised Denoising Network

Real-world off-the-shelf cameras are prone to capturing noise while recording LDR frames. This noise produces unwanted artifacts in both scenarios, i.e., first while aligning the neighboring frames by computing the optical flow between the frames and secondly on final reconstruction from these aligned frames. In order to reconstruct high-quality HDR frames, we require the corresponding LDR frames to be less noisy. In our method, we incorporate a denoising network that removes such imperfections from the noisy LDR frames. We call our self-supervised denoising blocks as ELDR blocks.

Self-Supervised paradigm has shown promising results in learning feature representation [16, 46], temporal coherency [38], image denoising [52], and many other tasks [25, 26, 55]. Inspired by this, we design a self-supervision based LDR frames denoising network that learns to create clean LDR frames from the noisy LDR video frames. For all our experimentation, we use Gaussian noise as the perturbation function to generate noisy LDR frames from the synthetic LDR frames as described in Equation 2, consistent with previous baselines [19]. Figure 2 shows the example of an overexposed LDR and the corresponding frame after the Gaussian noise addition.

$$L'_i = L_i + N(\mu, \sigma) \quad (2)$$

Our LDR frame denoise network consists of a series of convolution and deconvolution operations along with a skip connection between them following a U-Net [42] like structure. Each 2-D convolution operation is followed by a BatchNorm operation, ReLU activation, and a 2×2 Max-pooling layer to reach the bottleneck representation. Then the bottleneck feature map is upsampled using deconvolution layers. Figure 3 shows the architecture of our

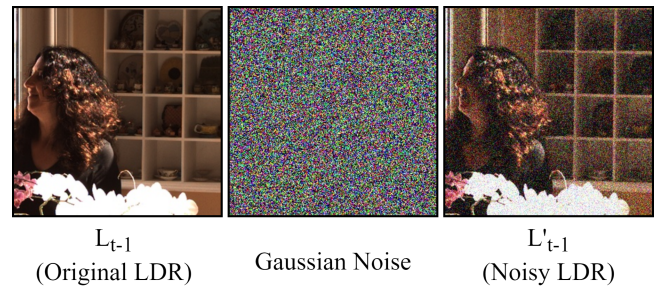


Figure 2: Visual comparison of noisy LDR frame L'_{t-1} generated by adding gaussian noise using Equation 2 to the synthetically generated LDR frames L_{t-1}

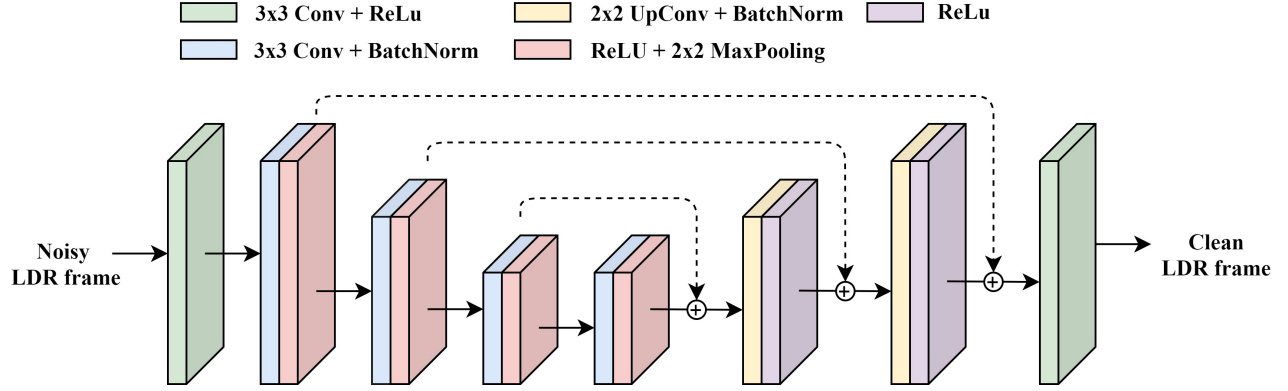


Figure 3: Architecture of our Denoising network

denoising network. In each iteration of the training procedure, we take the LDR frames (L_i), and we add perturbation to it according to Equation 2 and use these perturbed images as the input to the network. The network is trained to extract out the original clean LDR frames from all the added noise. Our proposed method consists of two such denoising networks, each for a different exposure. All the parameters are identical across both networks. The difference is that one network is trained on LDR frames with low exposures and another for LDR frames with high exposures. Formally, we train our denoising blocks using the $L1$ loss given below.

$$L'_{denoise} = ||\tilde{L}_i - L_i||_1 \quad (3)$$

4.2 Flow Network

In video-to-video synthesis tasks, object movements across frames are known to create temporal artifacts during the reconstruction. Visually incoherent frames with poor temporal coherency is observed if existing image synthesis is directly applied to videos without incorporating the temporal dynamics in the model. We address this by aligning all the input LDR frames with alternating exposure to a reference frame before using it for reconstructing the HDR frames. In order to achieve such an alignment, we first estimate the optical flow [29] between the consecutive LDR frames having alternating exposures, which is then used to warp the previous frame to the current frame.

Convolution neural network-based optical flow estimation was originally proposed by Dosovitskiy *et al.* [7], which directly generates a flow field from a pair of images. After this, many works have been proposed on neural network-based optical flow estimation [15, 37, 41]. However, most of these techniques are computationally expensive, and direct application of these methods in our case, would not be scalable for real-time estimation of HDR frames.

Therefore, we use a fine-tuned version of LiteFlowNet [14] in our proposed pipeline for optical flow estimation, which outperforms most other neural network-based flow estimation methods both in terms of speed and accuracy. After obtaining the clean version of LDR frames with alternating exposures, we compute the optical flow between these neighboring frames. Originally, LiteFlowNet [14] was trained to generate flow-maps between video-frames having

similar exposures. Directly using a pre-trained version of this LiteFlowNet [14] would result in inconsistencies due to the difference in exposures. In order to utilize this across different exposures, we fine-tune it by leaving it trainable during our end-to-end training procedure after initializing LiteFlowNet [14] with the pre-trained version.

4.3 GAN Based HDR Frame Generation

Network Architecture. We adopt the GAN based architecture for our HDR frame reconstruction proposed by [47]. The proposed generator network is based on encoder-decoder architecture, where the encoder first downsamples the image twice ($H \times W \rightarrow H/4 \times W/4$). The feature map is then passed through 8 Res-Blocks followed by two upsampling layers. Similar to [47], we use the instance norm layer. We warp a convolution layer, an instance-norm layer, and a ReLU activation layer into one basic unit. The Res-Block consists of 2 basic units stacked over each other. The discriminator consists of 5 convolution layers followed by two dense layers. To stabilize the training process, we use the spectral norm. By restricting our discriminative function to 1-Lipschitz, we prevent the gradient uninformative problem [58]. Figure 4 shows our proposed architecture. Let G and D denotes the generator and discriminator networks. Our generator network takes clean overexposed LDR (\tilde{L}_i) and an underexposed LDR (\tilde{L}_{i-1}) received after flow correction from the denoising networks and generates the current HDR frame (H_i).

$$H_i = G(\tilde{L}_i, \tilde{L}_{i-1}) \quad (4)$$

4.4 Objective Function

Tone Mapping. Kalantari *et al.* [19] argued that defining loss function in linear HDR domain underestimates the error in darker regions. The solution that they suggested is to convert HDR from linear domain to log domain [18, 53]. Consistent with the previous baselines [19], we also use differentiable μ -law function transformation denoted by T . We compute our loss on tonemapped HDR frames.

$$T_i = \frac{\log(1 + \mu H_i)}{\log(1 + \mu)} \quad (5)$$

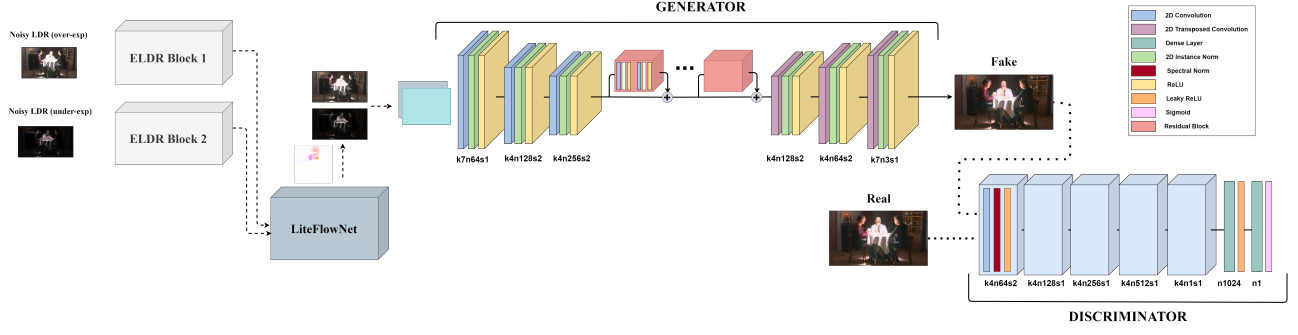


Figure 4: Our proposed method for HDR video generation consisting of two Denoising networks, a LiteFlowNet [14] model, and a final GAN based reconstruction model. Layers in both generator and discriminator can be identified by its color as described in the table on the right side. Each label of the layer follows the convention of k-kernel size-n-number of kernels-s-stride size.

L_1 Loss. Kalantari *et al.* [19] used l_1 loss computed between generated HDR frame and ground truth HDR frame to train the model. The authors also argued that the use of L_1 loss promotes sharpness in images as compared to L_2 loss. Again, consistent with the previous baselines, we also use L_1 loss in our model.

$$L_{l_1} = ||T_i - \tilde{T}_i||_1 \quad (6)$$

Adversarial Objective. Rather than discriminating with i^{th} ground truth HDR frame, Thasarthan and Nareri [47] proposed use of previous $(i - 1)^{th}$ frame. They argued that using a previous frame for discrimination generates temporally more coherent frames than frames generated using conventional adversarial loss. This adversarial loss reduces flickering artifacts in frames.

$$L_{adv} = \mathbb{E}_{(\tilde{T}_i, \tilde{T}_{i-1})} \log[D(\tilde{T}_i, \tilde{T}_{i-1})] + \mathbb{E}_{\tilde{T}_{i-1}} \log[1 - D(T_i, \tilde{T}_{i-1})] \quad (7)$$

Content and Style Losses. Frame reconstruction is also accompanied by other visual artifacts like blurriness and color mismatch. We incorporate content and style loss [43] to minimize visual artifacts. Let ϕ_i represent the activated feature map of j^{th} layer of pre-trained VGG-19. For our experiments, we use feature maps of 1^{st} to 5^{th} layers. We also use style loss to maintain spatial consistency in the generated HDR frame. Δ_j^ϕ represents Gram matrix of j^{th} feature map ϕ . Equation 8 represents content loss and Equation 9 represents style loss.

$$L_{content} = \mathbb{E}_j \left[\frac{1}{N_j} ||\phi_j(T_i) - \phi_j(\tilde{T}_i)||_1 \right] \quad (8)$$

$$L_{style} = \mathbb{E}_j \left[||\Delta_j^\phi(T_i) - \Delta_j^\phi(\tilde{T}_i)||_1 \right] \quad (9)$$

For our experiments we use $\lambda_{adv} = 5$, $\lambda_{content} = 1$, $\lambda_{style} = 1000$ and $\lambda_{l_1} = 30$, Equation 10 represents the overall loss function.

$$L_{rec} = \lambda_{adv}L_{adv} + \lambda_{content}L_{content} + \lambda_{style}L_{content} + \lambda_{style}L_{style} + \lambda_{l_1}L_{l_1} \quad (10)$$

Temporal Regularization. Finally, we incorporate explicit regularization for additional temporal stability [1, 6] between two

consecutive frames, which further helps in reducing blurriness in high motion frames. W represents warping function from our flow network and α is our regularization parameter, we set $\alpha = 0.3$.

$$L_{reg} = ||T_i - W(T_{i-1})||_2 \quad (11)$$

$$L_{total} = \alpha L_{rec} + (1 - \alpha)L_{reg} \quad (12)$$

5 TRAINING DETAILS

In this section, we discuss our training methodology and present the values of hyper-parameters. For all of our experiments, we used $\mu = 5000$ for tonemapping from linear to a logarithmic scale. We train our self-supervised denoising networks with L_{l_2} loss for 100 epochs. We train our GAN model with L_{rec} loss using a batch-size of 20 for 70 epochs, and then we fine-tune our network with L_{total} using a batch-size of 35 for 15 epochs. The training was performed entirely on a machine with Intel Core i7, 64GB of memory, and a GeForce RTX 2080-Ti GPU. It roughly takes six days to complete the training procedure (both denoising and GAN combined). Note that we freeze the weights for our denoising network before training our GAN model. We optimize our loss objective function using Adam optimizer with a learning rate of 10^{-4} for training self-supervised network and 10^{-4} for GANs with a batch size of 12. We use Leaky ReLU activation for the discriminator network [47], and for the rest of the network, we used ReLU activation. We used the spectral norm in the discriminator to stabilize our training procedure.

6 RESULTS

We compare our approach against the method of Kalantari *et al.* [20], which uses a patch-based mechanism for high dynamic range video generation and against the current state-of-the-art, Kalantari *et al.* [19] which is based on convolutional neural networks (CNNs). We used the publicly available source code for the patch-based method by Kalantari *et al.* [20] and Li *et al.* [27]. For CNN based approach by Kalantari *et al.* [19], the authors provided their results on only three scenes from the test set. Both the patch-based mechanism by Kalantari *et al.* [20] and Li *et al.* [27] takes roughly 1-2 hours for generating each of the frames with a resolution 1280×720 . Recent work on CNN based method by Kalantari *et al.* [19] showed that both patch-based method [20] and the method of Li *et al.* [27]

produce poor results on different scenes. Thus, visual comparison against patch-based method [20] and the method of Li *et al.* [27] is difficult and superfluous. Moreover, our proposed method has a training mechanism that is consistent with that of the recent CNN based model by Kalantari *et al.* [19] as explained in Section 5. Therefore, we only compare the visual results against CNN based model of Kalantari *et al.* [19].

6.1 Evaluation Metrics

To evaluate the performance of our end-to-end generative model we use PSNR [12], SSIM [59] and HDR-VDP-2 [34]. Given the ground truth image (gt) and the predicted image ($pred$), $PSNR(gt, pred)$ is defined as in equation 13 -

$$PSNR(gt, pred) = 10 \log_{10}(255^2 / MSE(gt, pred)) \quad (13)$$

where $MSE(gt, pred)$ is mean squared error between the ground truth image and predicted image having a size of $M \times N$ as in equation 14 -

$$MSE(gt, pred) = \frac{1}{M \cdot N} \sum_{i=1}^M \sum_{j=1}^N (gt_{ij} - pred_{ij})^2 \quad (14)$$

Higher the PSNR value better is the quality of the reconstructed image. The SSIM metric is also a well-known metric for measuring the visual quality of the reconstructed image. SSIM metric takes into account luminance, contrast and structural similarity into account and hence it is highly correlated with the human perception.

HDR-VDP-2 [34] is also a visual metric that compares the visibility score, i.e., the difference between gt and $pred$ with respect to an average observer and the degradation quality of $pred$ with respect to gt expressed as a mean opinion score.

6.2 Quantitative Comparison

We quantitatively compare our results against the methods of Kang *et al.* [22], the patch-based method of Kalantari *et al.* [20], and the current state-of-the-art by Kalantari *et al.* [19]. We select frames from the scenes of FISHING LONGSHOT, CAROUSEL FIREWORKS, and POKER FULLSHOT, which all comprise of the test set. We extract LDR frames with alternating exposures, as described in previous sections. Each frame has a resolution of 1920×1080 , but has a wide black border of 10 pixels around them, which we crop on-wards for quantitative comparison.

We evaluate the results on PSNR (Peak signal-to-noise ratio) and SSIM (Structural Similarity Index) in its tone-mapped domain as described in Equation 5. To further evaluate the quality of the generated HDR frames, we use HDR-VDP2 [35], which is designed

	Kalantari [20]	Kalantari [19]	Ours
PSNR	38.77	40.67	43.35
SSIM	-	0.78	0.83
HDR-VDP-2	62.12	74.15	77.19

Table 2: Quantitative comparison of our method against the patch based method of Kalantari *et al.* [20] and CNN based method by Kalantari *et al.* [19].

specifically to evaluate HDR images and videos. Table 2 shows all the values using these metrics computed and averaged across all the frames on test data. It can be seen from Table 2 that the proposed method outperforms the other existing approaches with respect to all the considered metrics.

6.3 Visual Comparisons

We compare the reconstructed HDR frames of our method, and the CNN based method of Kalantari *et al.* [19] on scenes in the test set. Figure 6 shows a detailed comparison of an HDR frame from a test video scene. The scene shows the FISHING LONGSHOT, which includes a bright region exposed by the sun (marked in the blue box) and a dark region having very low exposure (marked in red box). It can be clearly observed from the regions bounded by the blue and green color that the proposed method produces frames with much more dynamic range than that of Kalantari *et al.* [19]. On a close observation near the region of the sky (bounded in blue) in Figure 6, it can be seen that our method reconstructs the details of the clouds, while the one produced by the method of Kalantari *et al.* [19] loses the content and reconstructs an over-exposed frame. Overall, from Figure 6 it can be seen that our method generates HDR frames with much more details in regions of both the high and low exposure areas.

Figure 5 and Figure 7 compare our approach against the CNN based method by Kalantari *et al.* [19] on the scenes of CAROUSEL FIREWORKS and FISHING LONGSHOT respectively, which were not part of the training set. We selected those frames to form the video scene with significant motion in-between the adjacent frames i.e. high motion frames. As evident from the frames of CAROUSEL



Figure 5: Visual Comparison of our generated HDR frames having high motion from CAROUSEL FIREWORKS scene in test data against Kalantari *et al.* [19].

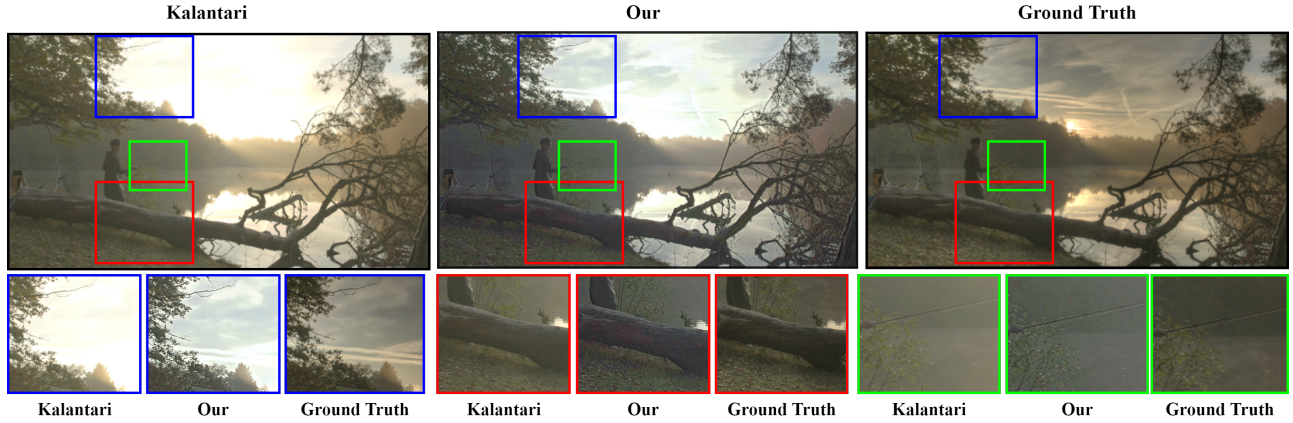


Figure 6: Visual Comparison of the our generated HDR frames from a scene of FISHING LONGSHOT in the test data against Kalantari *et al.* [19]. Identical regions of comparison are all grouped in the same color.

FIREWORKS in Figure 5, CNN based method by Kalantari *et al.* [19] generates tearing artifacts in moving parts of the person in the frame. It also produces blurred frames with ghosting artifacts in the scene of FISHING LONGSHOT in Figure 7 marked by red arrows.

6.4 Denoising Network

We begin by showing the results of the denoising network (ELDR Blocks), which is trained in a self-supervised manner on the same training set scenes. We extract LDR frames with alternating exposures from the HDR videos, as described in Section 3. For each LDR frame having alternating exposures, we add Gaussian noise

with varied signal-to-noise ratios (SNR), which we described in Section 4.1. Figure 8 shows the results of a clean LDR frame generated by our denoising network from a noisy LDR frame of a scene, which was earlier described in Figure 2. In general, we observe that the generated LDR frames have a coherent texture with sharp features as compared to the noisy LDR frames. The use of L_1 loss function in the ELDR blocks can be accounted for the above observation.

7 ABLATION STUDY

Importance of Separate LDR Denoising Blocks. To study the significance of these ELDR blocks, we remove these blocks from our overall pipeline and re-train the model. It is evident from Table 3 and Figure 9 that both visual quality and metric-wise, removal of denoising network have a significant effect on the performance of our method. We observe a notable drop in the PSNR, SSIM, and HDR-VDP2 [35] values. We find HDR frames generated directly from noise embedded LDRs to be blurry with less detailed reconstruction as compared to our complete approach, which generates crisp details as shown in Figure 9. Thus, creating a two-stage network where noise removal and reconstruction of HDR videos are performed separately has shown to perform better than a single network performing both the tasks. Moreover, the generated intermediate clean

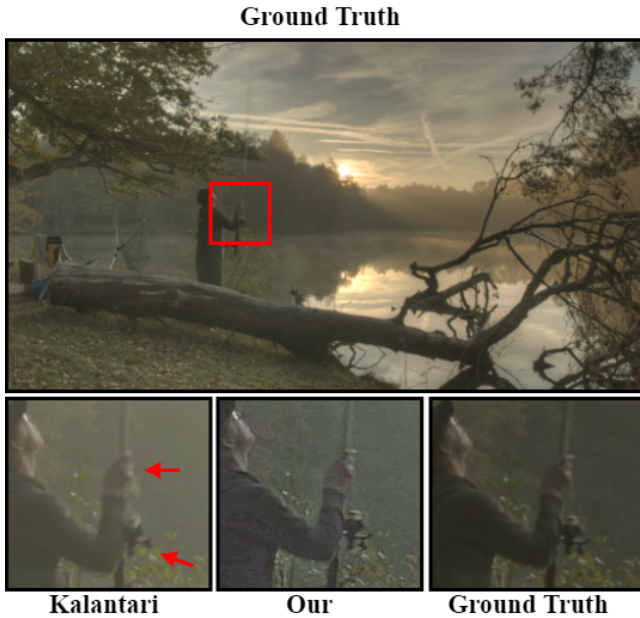


Figure 7: Visual Comparison of our generated HDR frames having high motion from FISHING LONGSHOT scene in test data against Kalantari *et al.* [19].



Figure 8: Visual comparison of a reconstructed clean LDR frame using denoising network from a noisy LDR frame of a scene used previously in Figure 2

LDR frames add more interpretability in terms of noise removal to our model as compared to previous baselines [18, 19].

	Without denoising net	Ours (Complete)
PSNR	41.39	43.35
SSIM	0.76	0.83
HDR-VDP-2	73.87	77.19

Table 3: Quantitative comparison of our complete approach to our method without denoising network. Removing the denoising network clearly drops the performance on all the mentioned metrics.

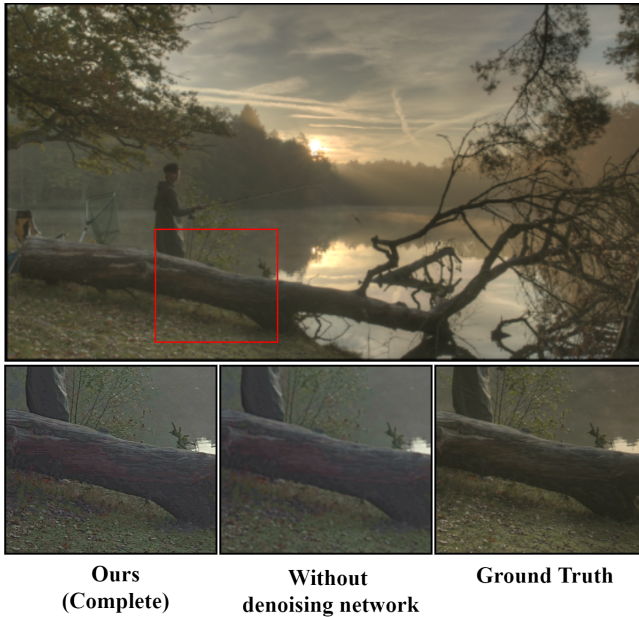


Figure 9: Visual comparison of our complete approach to our method without the denoising network. Removing the denoising network leads to reconstruction of HDR frames having poor quality with less details.

8 CONCLUSION

In this paper, we proposed a temporally stable GAN-based HDR video reconstruction network that reconstructs HDR videos from LDR sequences with alternating exposures. Our method incorporates a separate LDR denoising network for extracting clean LDR frames, and we showed that creating separate denoising and reconstruction network outperforms a single network that performs both the tasks. We first align the neighboring alternating exposure frames using the LiteFlowNet [14] to generate temporally coherent frames. Training our model over a joint objective consisting of L_1 loss, style-aware content losses [43] and augmented GAN loss [47] helped in minimizing the visual artifacts. Further, we fine-tune our model on a temporal stability based regularization term

to further reduce the tearing and ghosting artifacts due to temporal incoherence. We perform all our experimentation consistent with the previous baselines, and we demonstrate that our method outperforms the previous baselines both visually and metric-wise.

We believe that there is a great scope for further improvement in terms of better colors, more dynamic range, and in overall visual quality. In the future, we would like to further test our proposed method on larger datasets of HDR videos as and when they become available.

ACKNOWLEDGMENTS

We would like to thank Science and Engineering Research Board (SERB) Core Research Grant for supporting our work.

REFERENCES

- [1] Nicolas Bonneel, James Tompkin, Kalyan Sunkavalli, Deqing Sun, Sylvain Paris, and Hanspeter Pfister. 2015. Blind Video Temporal Consistency. *ACM Trans. Graph.* 34, 6, Article 196 (Oct. 2015), 9 pages. <https://doi.org/10.1145/2816795.2818107>
- [2] Vladimir Brajovic and Takeo Kanade. 1996. A sorting image sensor: An example of massively parallel intensity-to-time processing for low-latency computational sensors. In *Proceedings of IEEE International Conference on Robotics and Automation*, Vol. 2. IEEE, 1638–1643.
- [3] PE Debevec and J Malik. 1997. Recovering high dynamic range radiance maps from photographs: Proceedings of the 24th Annual Conference on Computer Graphics and Interactive Techniques. *Los Angeles, USA: SIGGRAPH* (1997).
- [4] Paul E Debevec and Jitendra Malik. 2008. Recovering high dynamic range radiance maps from photographs. In *ACM SIGGRAPH 2008 classes*. 1–10.
- [5] Gabriel Eilertsen, Joel Kronander, Gyorgy Denes, Rafal K Mantiuk, and Jonas Unger. 2017. HDR image reconstruction from a single exposure using deep CNNs. *ACM Transactions on Graphics (TOG)* 36, 6 (2017), 1–15.
- [6] Gabriel Eilertsen, Rafal K. Mantiuk, and Jonas Unger. 2019. Single-Frame Regularization for Temporally Stable CNNs. *2019 IEEE/CVF Conference on Computer Vision and Pattern Recognition (CVPR)* (2019). <https://doi.org/10.1109/cvpr.2019.01143>
- [7] Philipp Fischer, Alexey Dosovitskiy, Eddy Ilg, Philip Häusser, Caner Hazırbaşı, Vladimir Golkov, Patrick van der Smagt, Daniel Cremers, and Thomas Brox. 2015. FlowNet: Learning Optical Flow with Convolutional Networks. *arXiv:1504.06852 [cs.CV]*
- [8] Jan Froehlich, Stefan Grandinetti, Bernd Eberhardt, Simon Walter, Andreas Schilling, and Harald Brendel. 2014. Creating cinematic wide gamut HDR-video for the evaluation of tone mapping operators and HDR-displays. In *Digital Photography X*, Vol. 9023. International Society for Optics and Photonics, 90230X.
- [9] Orazio Gallo, Alejandro Troccoli, Jun Hu, Kari Pulli, and Jan Kautz. 2015. Locally non-rigid registration for mobile HDR photography. In *Proceedings of the IEEE Conference on Computer Vision and Pattern Recognition Workshops*. 49–56.
- [10] Yulia Gryaditskaya, Tania Pouli, Erik Reinhard, Karol Myszkowski, and Hans-Peter Seidel. 2015. Motion aware exposure bracketing for HDR video. In *Computer Graphics Forum*, Vol. 34. Wiley Online Library, 119–130.
- [11] Samuel W Hasinoff, Dillon Sharlet, Ryan Geiss, Andrew Adams, Jonathan T Barron, Florian Kainz, Jiawen Chen, and Marc Levoy. 2016. Burst photography for high dynamic range and low-light imaging on mobile cameras. *ACM Transactions on Graphics (TOG)* 35, 6 (2016), 1–12.
- [12] A. Horé and D. Ziou. 2010. Image Quality Metrics: PSNR vs. SSIM. In *2010 20th International Conference on Pattern Recognition*. 2366–2369. <https://doi.org/10.1109/ICPR.2010.579>
- [13] Jun Hu, Orazio Gallo, Kari Pulli, and Xiaobai Sun. 2013. HDR deghosting: How to deal with saturation?. In *Proceedings of the IEEE Conference on Computer Vision and Pattern Recognition*. 1163–1170.
- [14] Tak-Wai Hui, Xiaoou Tang, and Chen Change Loy. 2018. LiteFlowNet: A Lightweight Convolutional Neural Network for Optical Flow Estimation. In *Proceedings of IEEE Conference on Computer Vision and Pattern Recognition (CVPR)*. 8981–8989.
- [15] E. Ilg, N. Mayer, T. Saikia, M. Keuper, A. Dosovitskiy, and T. Brox. 2017. FlowNet 2.0: Evolution of Optical Flow Estimation with Deep Networks. In *IEEE Conference on Computer Vision and Pattern Recognition (CVPR)*. <http://lmb.informatik.uni-freiburg.de/Publications/2017/IMKDB17>
- [16] Simon Jenni and Paolo Favaro. 2018. Self-Supervised Feature Learning by Learning to Spot Artifacts. *CoRR abs/1806.05024* (2018). [arXiv:1806.05024](https://arxiv.org/abs/1806.05024)
- [17] Justin Johnson, Alexandre Alahi, and Li Fei-Fei. 2016. Perceptual losses for real-time style transfer and super-resolution. In *European conference on computer vision*. Springer, 694–711.

- [18] Nima Khademi Kalantari and Ravi Ramamoorthi. 2017. Deep high dynamic range imaging of dynamic scenes. *ACM Trans. Graph.* 36, 4 (2017), 144–1.
- [19] Nima Khademi Kalantari and Ravi Ramamoorthi. 2019. Deep HDR Video from Sequences with Alternating Exposures. In *Computer Graphics Forum*, Vol. 38. Wiley Online Library, 193–205.
- [20] Nima Khademi Kalantari, Eli Shechtman, Connelly Barnes, Soheil Darabi, Dan B Goldman, and Pradeep Sen. 2013. Patch-based high dynamic range video. *ACM Trans. Graph.* 32, 6 (2013), 202–1.
- [21] Sing Bing Kang, Matthew Uyttendaele, Simon Winder, and Richard Szeliski. 2003. High dynamic range video. *ACM Transactions on Graphics (TOG)* 22, 3 (2003), 319–325.
- [22] Erum Arif Khan, Ahmet Oguz Akyuz, and Erik Reinhard. 2006. Ghost removal in high dynamic range images. In *2006 International Conference on Image Processing*. IEEE, 2005–2008.
- [23] Joel Kronander, Stefan Gustavson, Gerhard Bonnet, and Jonas Unger. 2013. Unified HDR reconstruction from raw CFA data. In *IEEE international conference on computational photography (ICCP)*. IEEE, 1–9.
- [24] Joel Kronander, Stefan Gustavson, Gerhard Bonnet, Anders Ynnerman, and Jonas Unger. 2014. A unified framework for multi-sensor HDR video reconstruction. *Signal Processing: Image Communication* 29, 2 (2014), 203–215.
- [25] Zihang Lai and Weidi Xie. 2019. Self-supervised Learning for Video Correspondence Flow. *CoRR* abs/1905.00875 (2019). arXiv:1905.00875 <http://arxiv.org/abs/1905.00875>
- [26] Samuli Laine, Tero Karras, Jaakko Lehtinen, and Timo Aila. 2019. High-Quality Self-Supervised Deep Image Denoising. In *Advances in Neural Information Processing Systems* 32, H. Wallach, H. Larochelle, A. Beygelzimer, F. d'Alché-Buc, E. Fox, and R. Garnett (Eds.). Curran Associates, Inc., 6970–6980. <http://papers.nips.cc/paper/8920-high-quality-self-supervised-deep-image-denoising.pdf>
- [27] Yuelong Li, Chul Lee, and Vishal Monga. 2016. A maximum a posteriori estimation framework for robust high dynamic range video synthesis. *IEEE Transactions on Image Processing* 26, 3 (2016), 1143–1157.
- [28] Ziwei Liu, Lu Yuan, Xiaoou Tang, Matt Uyttendaele, and Jian Sun. 2014. Fast burst images denoising. *ACM Transactions on Graphics (TOG)* 33, 6 (2014), 1–9.
- [29] Bruce D. Lucas and Takeo Kanade. 1981. An Iterative Image Registration Technique with an Application to Stereo Vision. In *Proceedings of the 7th International Joint Conference on Artificial Intelligence - Volume 2* (Vancouver, BC, Canada) (IJCAI'81). Morgan Kaufmann Publishers Inc., San Francisco, CA, USA, 674–679.
- [30] Kede Ma, Hui Li, Hongwei Yong, Zhou Wang, Deyu Meng, and Lei Zhang. 2017. Robust multi-exposure image fusion: A structural patch decomposition approach. *IEEE Transactions on Image Processing* 26, 5 (2017), 2519–2532.
- [31] Stephen Mangiat and Jerry Gibson. 2011. Spatially adaptive filtering for registration artifact removal in HDR video. In *2011 18th IEEE International Conference on Image Processing*. IEEE, 1317–1320.
- [32] Steve Mann, Corey Manders, and James Fung. 2002. Painting with looks: Photographic images from video using quantitative processing. In *Proceedings of the tenth ACM international conference on Multimedia*. 117–126.
- [33] S Mann and R Picard. 1994. Being undigital with digital cameras. *MIT Media Lab Perceptual* 1 (1994), 2.
- [34] Rafa Mantiuk, Kil Joong Kim, Allan G. Rempel, and Wolfgang Heidrich. 2011. HDR-VDP-2: A Calibrated Visual Metric for Visibility and Quality Predictions in All Luminance Conditions. *ACM Trans. Graph.* 30, 4, Article 40 (July 2011), 14 pages. <https://doi.org/10.1145/2010324.1964935>
- [35] Rafal Mantiuk, Kil Joong Kim, Allan G. Rempel, and Wolfgang Heidrich. 2011. HDR-VDP-2: A Calibrated Visual Metric for Visibility and Quality Predictions in All Luminance Conditions. 30, 4, Article 40 (July 2011), 14 pages. <https://doi.org/10.1145/2010324.1964935>
- [36] Demetris Marnerides, Thomas Bashford-Rogers, Jonathan Hatchett, and Kurt Debattista. 2018. ExpandNet: A deep convolutional neural network for high dynamic range expansion from low dynamic range content. In *Computer Graphics Forum*, Vol. 37. Wiley Online Library, 37–49.
- [37] Daniel Maurer and Andrés Bruhn. 2018. ProFlow: Learning to Predict Optical Flow. arXiv:1806.00800 [cs.CV]
- [38] Hossein Mobahi, Ronan Collobert, and Jason Weston. 2009. Deep Learning from Temporal Coherence in Video. In *Proceedings of the 26th Annual International Conference on Machine Learning* (Montreal, Quebec, Canada) (ICML '09). Association for Computing Machinery, New York, NY, USA, 737–744. <https://doi.org/10.1145/1553374.1553469>
- [39] Shree K Nayar and Tomoo Mitsunaga. 2000. High dynamic range imaging: Spatially varying pixel exposures. In *Proceedings IEEE Conference on Computer Vision and Pattern Recognition. CVPR 2000 (Cat. No. PR00662)*, Vol. 1. IEEE, 472–479.
- [40] Tae-Hyun Oh, Joon-Young Lee, Yu-Wing Tai, and In So Kweon. 2014. Robust high dynamic range imaging by rank minimization. *IEEE transactions on pattern analysis and machine intelligence* 37, 6 (2014), 1219–1232.
- [41] A. Ranjan and M. J. Black. 2017. Optical Flow Estimation Using a Spatial Pyramid Network. In *2017 IEEE Conference on Computer Vision and Pattern Recognition (CVPR)*. 2720–2729.
- [42] Olaf Ronneberger, Philipp Fischer, and Thomas Brox. 2015. U-Net: Convolutional Networks for Biomedical Image Segmentation. arXiv:1505.04597 [cs.CV]
- [43] Artiom Sanakoyeu, Dmytro Kotovenko, Sabine Lang, and Bjorn Ommer. 2018. A Style-Aware Content Loss for Real-time HD Style Transfer. In *Proceedings of the European Conference on Computer Vision (ECCV)*.
- [44] Ulrich Seger, Uwe Apel, and Bernd Höflinger. 1999. HDRC-imagers for natural visual perception. *Handbook of Computer Vision and Application* 1 (1999), 223–235.
- [45] Pradeep Sen, Nima Khademi Kalantari, Maziar Yaesoubi, Soheil Darabi, Dan B Goldman, and Eli Shechtman. 2012. Robust patch-based hdr reconstruction of dynamic scenes. *ACM Trans. Graph.* 31, 6 (2012), 203–1.
- [46] Karen Simonyan and Andrew Zisserman. 2014. Two-Stream Convolutional Networks for Action Recognition in Videos. In *Proceedings of the 27th International Conference on Neural Information Processing Systems - Volume 1* (Montreal, Canada) (NIPS'14). MIT Press, Cambridge, MA, USA, 568–576.
- [47] Harrish Thasarathan, Kamyar Nazeri, and Mehran Ebrahimi. 2019. Automatic temporally coherent video colorization. In *2019 16th Conference on Computer and Robot Vision (CRV)*. IEEE, 189–194.
- [48] MD Tocci, C Kiser, N Tocci, and P Sen. [n.d.]. A Versatile HDR Video Production System. *ACM TOG* 30 (4), 41: 1–41: 10 (Jul 2011).
- [49] Michael D Tocci, Chris Kiser, Nora Tocci, and Pradeep Sen. 2011. A versatile HDR video production system. *ACM Transactions on Graphics (TOG)* 30, 4 (2011), 1–10.
- [50] Anna Tomaszewska and Radoslaw Mantiuk. 2007. Image registration for multi-exposure high dynamic range image acquisition. (2007).
- [51] Greg Ward. 2003. Fast, robust image registration for compositing high dynamic range photographs from hand-held exposures. *Journal of graphics tools* 8, 2 (2003), 17–30.
- [52] Jun Xu, Yuan Huang, Ming-Ming Cheng, Li Liu, Fan Zhu, Zhou Xu, and Ling Shao. 2019. Noisy-As-Clean: Learning Self-supervised Denoising from the Corrupted Image. arXiv:1906.06878 [cs.CV]
- [53] Jinsong Zhang and Jean-François Lalonde. 2017. Learning High Dynamic Range from Outdoor Panoramas. In *IEEE International Conference on Computer Vision*.
- [54] Li Zhang, Alok Deshpande, and Xin Chen. 2010. Denoising vs. deblurring: HDR imaging techniques using moving cameras. In *2010 IEEE Computer Society Conference on Computer Vision and Pattern Recognition*. IEEE, 522–529.
- [55] Richard Zhang, Phillip Isola, and Alexei A. Efros. 2016. Colorful Image Colorization. *CoRR* abs/1603.08511 (2016). arXiv:1603.08511 <http://arxiv.org/abs/1603.08511>
- [56] Hang Zhao, Boxin Shi, Christy Fernandez-Cull, Sai-Kit Yeung, and Ramesh Raskar. 2015. Unbounded high dynamic range photography using a modulo camera. In *2015 IEEE International Conference on Computational Photography (ICCP)*. IEEE, 1–10.
- [57] Jinghong Zheng, Zhengguo Li, Zijian Zhu, Shiqian Wu, and Susanto Rahardja. 2013. Hybrid patching for a sequence of differently exposed images with moving objects. *IEEE Transactions on Image Processing* 22, 12 (2013), 5190–5201.
- [58] Zhiming Zhou, Jiadong Liang, Yuxuan Song, Lantao Yu, Hongwei Wang, Weinan Zhang, Yong Yu, and Zhihua Zhang. 2019. Lipschitz Generative Adversarial Nets. *CoRR* abs/1902.05687 (2019). arXiv:1902.05687 <http://arxiv.org/abs/1902.05687>
- [59] Zhou Wang, A. C. Bovik, H. R. Sheikh, and E. P. Simoncelli. 2004. Image quality assessment: from error visibility to structural similarity. *IEEE Transactions on Image Processing* 13, 4 (2004), 600–612. <https://doi.org/10.1109/TIP.2003.819861>